Analysis for Laterally Loaded Offshore Piles in Marine Clay

S. Jeong[1], and Y. Kim[2]
[1]*Department of Civil, and Environmental Engineering, Yonsei Univ., Seoul, Republic of Korea*
[2]*Centre for Offshore Foundation Systems, Oceans Graduate School, Univ. of Western Australia, Crawley, WA, Australia*
[1]*E-mail*: soj9081@yonsei.ac.kr

ABSTRACT: The load distribution and deformation of offshore drilled shafts under lateral loading in Incheon grand bridge are investigated by experimental field loading tests and lateral load-transfer approach through p-y curve analysis. The main focus is on improved wedge failure model developed by considering three-dimensional combination forces and new hyperbolic p-y criterion. Through comparisons with field case studies, it is found that the rigidity of the drilled shaft is a critical factor in drilled shafts in marine clay, and the methodology proposed in this study yields more accurate and realistic results considering pile-soil interaction for laterally loaded drilled shafts in marine clay.

KEYWORDS: Drilled shaft, Lateral loading, Marine clay, p-y curve, Wedge failure model, Pile rigidity

1. INTRODUCTION

In South Korea, large diameter drilled shafts are commonly used as main foundation elements for long span bridges and high-rise buildings; where high resistance against lateral loads are required. Much work has been done on laterally loaded piles. The p-y method developed by Matlock (1970), Reese (1977), O'Neill (1984) and Briaud (1984, 1997) for small diameter piles is the most commonly used procedure for the analysis of laterally loaded piles. The confidence in this method is derived from the fact that the p-y curves have been obtained from few full-scale field tests. These traditional models are well known as semi-empirical approaches in which the soil response is represented by independent nonlinear springs at discrete locations. Moreover, most p-y curves used in practice are based on the results of lateral load test on relatively small diameter piles (e.g., Matlock: 0.33 m diameter steel-pipe piles; Reese et al.: 0.61 m diameter steel-piles; Reese and Welch: 0.90 m diameter drilled shaft). The main limitation of this p-y approach is that p-y curves are not unique. Instead the p-y relationships for a given soil can be significantly influenced by pile properties and soil continuity (Jung et al. 2017; Kim 2018; Kim et al. 2018). The discrete representation implies that the continuity of the soil mass and of the soil-pile interaction is not properly considered. Thus, a new method is required to overcome the limitations of the traditional p-y method.

The overall objective of this study is to develop the improved wedge failure model for predicting the ultimate soil resistance by considering a 3D combination of forces and a new hyperbolic p-y criterion that will apply to drilled shafts. To that end, a series of lateral load tests were performed. The validity of this study was tested by field case studies. In addition, the effect of rigidity between the pile-soil was investigated based on parametric study.

2. LATERAL FIELD LOADING TEST

Lateral field loading tests were conducted at the Incheon bridge site in western coast of the Korean peninsula. Due to the complexity of pile-soil interaction, a comprehensive geotechnical investigation was carried out to determine the soil profile and properties at the test site accurately. Figure 1 schematically states the concept of laterally loaded pile in soil. This investigation included five boreholes (W107, W108, W117, E36, E39), with conventional sampling near the test piles. Figure 2 shows an idealization of the subsurface profile with borehole and shaft embedment for the test piles based on the results of the field and laboratory tests. The properties of the soil layers based on the site investigations are summarized in Table 1.

To investigate the lateral load transfer curves of piles placed in clay, full-scale field load tests were performed on six instrumented piles as summarized in Table 2. Figure 3 shows an idealization of the subsurface profile with borehole and shaft embedment for the test piles based on the results of field and laboratory tests. The steel piles (LTP-1, LTP-2 and LTP-3) had an outer diameter of 1.016m and a wall thickness of 16mm. Each pile was driven such that 1.0m of the pile remained above the ground surface. The final depth of the driven piles was recorded as 25.6m. The drilled shafts (LTP-4, LTP-5, LTP-6) had a 2.4m diameter, 9.1m above the ground surface, and 44.3m and 45.9m embedment length for Case 4, and for Case 5 and 6. Excavation was performed by the reverse circulation drilling (RCD) method. Very large steel-reinforcement was used in order to ensure that structural failure would not occur. The reinforcing cage consisted of 34 D41 longitudinal bars (41mm) with a D19 (19mm) transverse spiral at an 11cm pitch over the pile length. For the lateral load test, the load was increased substantially up and down in 60 min load steps. This procedure was repeated until the anticipated design load was reached and a total of seven load increments were applied.

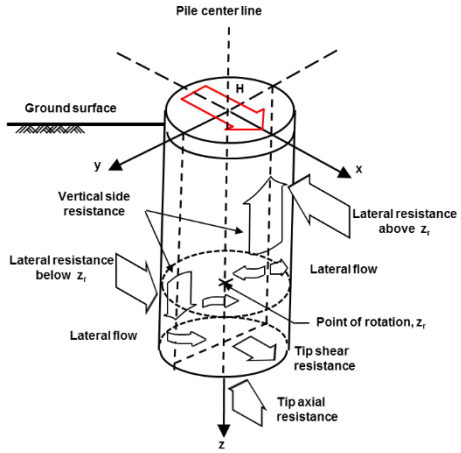

Figure 1 Schematic of laterally loaded pile in soil

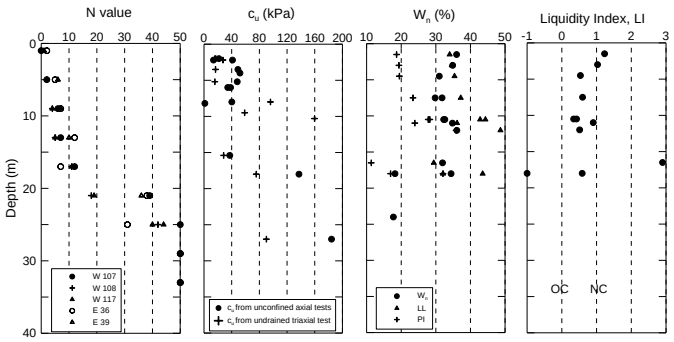

Figure 2 Soil profile; (a) soil profile of test site, (b) results from field and laboratory tests

Table 1 Soil properties (field test)

Soil	Clay	Silty clay	Residual soil	Weathered rock	Soft rock
γ_{sat} (kN/m^3)	17.5	17.8	17.8	20.2	20.5
N value	1 ~ 7	12 ~ 19	44	50/15~	100
$C_{u,avr}$ (kPa)	30	60	-	-	-
ϕ (Deg.)	-	-	34	32	33
PI	25 ~ 35	35 ~ 40	-	-	-
K_c	565	450	-	-	-
μ_s	0.3	0.3	0.3	0.25	0.25
OCR	0 ~ 2	< 2	-	-	-
ε_{50}	0.02	-	-	-	-

Table 2 Pile properties (field test)

Margins	Steel pile	Drilled shaft
Diameter (m)	1.02	2.4
Thickness (m)	0.016	-
Pile depth (m)	26.6	44.3
γ (kN/m^3)	72	25
E_p (kPa)	2.0×10^8	2.6×10^7
I_p	0.0063	1.629
Pile number	LTP-1, LTP-2, LTP-3	LTP-4, LTP-5, LTP-6

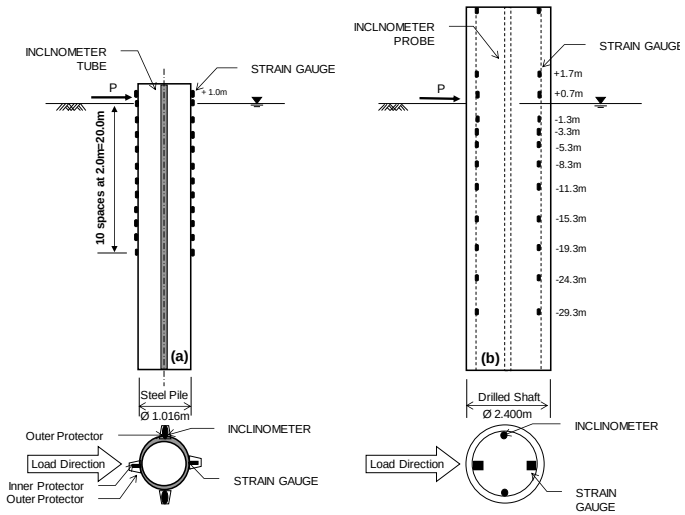

Figure 3 Field load test instruments; (a) steel pile, (b) drilled-shaft

The main advantage of laboratory pile load tests over field pile load tests is the capability to more detailed control the test conditions. Four laboratory load tests were also performed to complement the field load tests by varying the soil properties and the pile-soil rigidity. The test pit used for these experiments is located in the Geotechnical Testing Laboratory at Yonsei University, Korea. As shown in Figure 4, these tests were performed in a transparent acrylic cylinder. The size of the cylinder is considered to be large enough to minimize the influence of the boundary effect.

The laboratory load tests were conducted on two model piles; one short and rigid, and long and flexible according to the pile-soil rigidity criterion (Broms 1964; Randolph 1981). The diameters are set to 32mm. The soil used in the laboratory was some of the marine deposit from the field load test site. To create the testing soil in the laboratory, the proportions of water and clay soil in the simulated mixture were based on the field soil properties obtained from the load test field sites. Laboratory vane tests were conducted to determine the undrained shear strength (c_u) of the test soil at several depths. The test soil was prepared at two different undrained shear strengths (18kPa and 42kPa) by controlling the water content. A summary of the model tests is stated in Table 3.

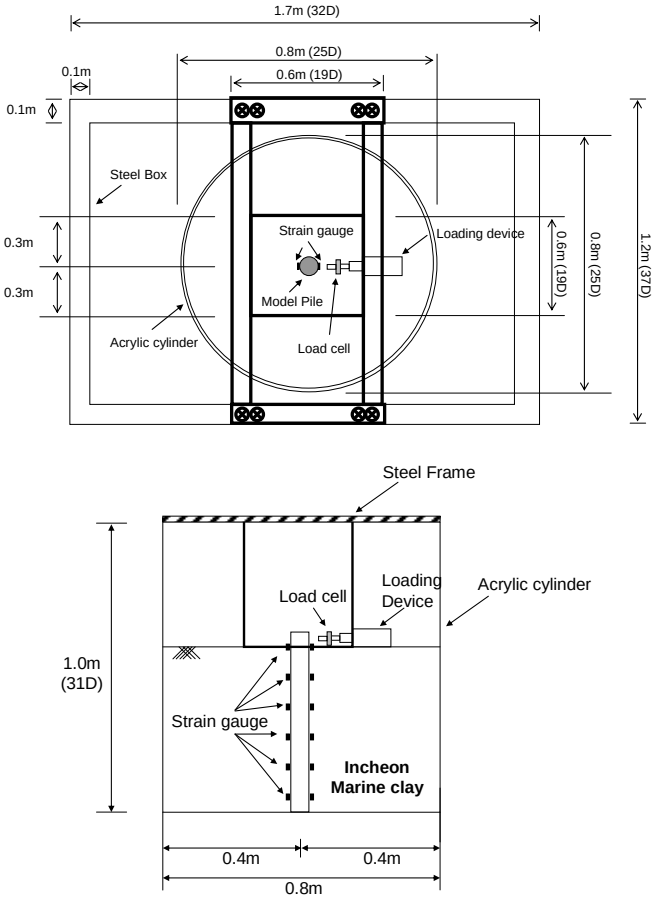

Figure 4 Laboratory test devices; (a) plane view, (b) section view

Table 3 Material properties : laboratory test

Pile No.	Pile type	c_u (kPa)	Pile depth (mm)	βL (m^{-1})	E_pI_p (kN-m^2)
MP-1	Short	18	400	1.1	4.36
MP-2	Short	42	400	1.6	4.36
MP-3	Long	18	650	2.4	4.36
MP-4	Long	42	650	3.0	4.36

Figure 5 presents the load-displacement response measured at the top of each pile in field tests and laboratory tests. As shown in Figure 4(a), it can be seen that it shows a similar shape of lateral load-displacement curve for steel piles (LPT 1 ~ LPT 3), drilled shafts (LPT 4 ~ LPT 6). As shown in Figure 4(b), the lateral displacement under same undrained shear strength decreased with the increasing pile length, whereas it decreased as the undrained shear strength increased. In addition, the rate of change of lateral displacement due to the change of the undrained shear strength is larger in the short pile than in the long pile.

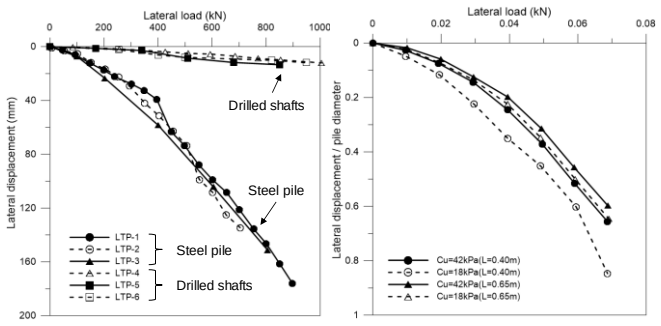

Figure 5 Load-displacement curves; (a) field test, (b) laboratory test

3. HYPERBOLIC p-y CURVE MODEL FOR CLAY

In this study, the shape of the p-y curves obtained in the field and in the laboratory is in general agreement with the hyperbolic function. Therefore, the following p-y curve is introduced:

$$p = \frac{y}{\frac{1}{K} + \frac{y}{p_u}} \tag{1}$$

where, y is the lateral displacement of pile, p_u is the ultimate soil resistance per unit length; and K is the initial tangent slope to the p-y curve. The shape of the hyperbolic curve is in general controlled by the values of p_u and K, and thus these numerical values are developed based on both load test and theoretical derivation results.

3.1 Initial slope (K) of p-y curves

In most of the previous models (Vesic, 1961; Bowles, 1988; Ashford, 2003), the subgrade reaction modulus K of the p-y curve is usually estimated from the soil modulus of elasticity (E_s). To account for the effect of pile diameter on the subgrade reaction modulus, Carter (1984) and Ling (1988) suggested a linear relationship between the subgrade reaction modulus and the pile diameter by using fitting parameters as following:

$$K = \frac{1.0E_s}{(1-\mu_s^2)} \frac{D}{D_{ref}} \left[\frac{E_s D^4}{E_p I_p}\right]^{\frac{1}{12}} \tag{2}$$

In this study, the generalized function for K is modified by introducing Equation 2 to consider the effect of pile diameter and the site specific soil conditions.

$$K = i \frac{E_s}{(1-\mu_s^2)} \frac{D}{D_{ref}} \left[\frac{E_s D^4}{E_p I_p}\right]^{j} \tag{3}$$

where μ_s is the Poisson's ratio of the soil; D is the pile diameter (m); D_{ref} is 1.0m; E_pI_p is the flexural rigidity of pile (kN-m^2); E_s is the soil modulus of elasticity (kN/m^2) which was represented by $K_c \times c_u$ (USACE, 1990); c_u is the undrained shear strength; K_c is the correlation factor that depends on the overconsolidation ratio and plasticity index; and i, j are the fitting parameters. Linear regression analysis was used to obtain the best-fit values of i and j.

Through linear regression analysis, the following empirical equation for K was obtained:

$$K = 16.01 \frac{E_s}{(1-\mu_s^2)} \frac{D}{D_{ref}} \left[\frac{E_s D^4}{E_p I_p}\right]^{0.8} \tag{4}$$

3.2 Ultimate soil resistance (p_u) of p-y curve

Studies on constructing the p_u has been made to date, significantly by using the pressuremeter test (PMT) curve (Briaud et al. 1985, Briaud 1997) and force equilibrium on a passive soil wedge (Reese et al. 1975), upper-bound method of plasticity on a conical soil wedge (Murff and Hamilton 1993) and a "strain wedge" mode of soil failure (Ashour and Norris 2000). Based on the literature review, three-dimensional passive wedge of soil developing in front of the pile does account for soil continuity and soil-pile interaction (Reese, 1983; Ashour, 2000, Liang 2009). This concept is adopted and improved to represent the lateral deformation of the soil mass in this study. This solution takes into consideration the true three-dimensional behaviours. It considers the development of three-dimensional normal and shear stresses along the circumference of the pile surface as well as a three-dimensional soil failure wedge. The ultimate soil resistance is then obtained from the detailed consideration of the force and moment equilibrium conditions. Figure 6 shows the behaviour of pile as one structural element.

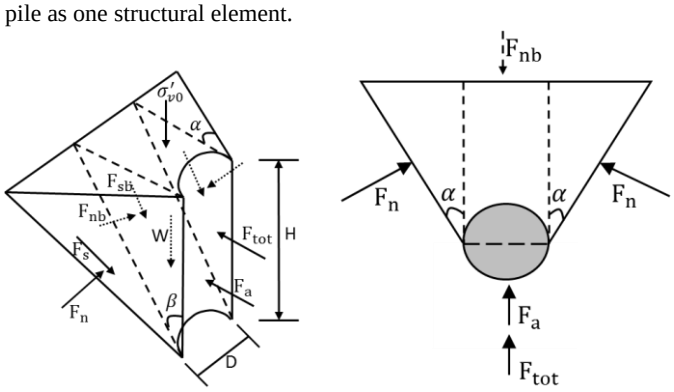

Figure 6 Three-dimensional wedge failure mode; (a) pile-soil system, (b) section view

Ashour and Norris (2000) showed that the angle of the wedge shape is associated with the effective friction angle (φ') of the soil, and therefore, an effective stress analysis can be employed with clay soil. Based on this approach, an effective stress analysis is incorporated in this study. It is important to note that the effective stress analysis with clay is to define the three-dimensional passive wedge shape (angle of α and θ) based on the more appropriate effective friction angle, represented by the plasticity index (Figure 7). As a result, the values of the wedge shape are not constant in clay soil, as assumed by Reese (1958, 1983), and the wedge shaft is thus dependent on the effective friction angle. Figure 8 shows the relationship between the results assessed with different fanning angles and the field results in this study. According to these results, the fanning angle (α) of clay is taken to be $\varphi'/5$. Then, the bottom angle (θ) of the three-dimensional wedge is determined to be $45^\circ + \varphi'/2$ by the Mohr-Coulomb failure criterion.

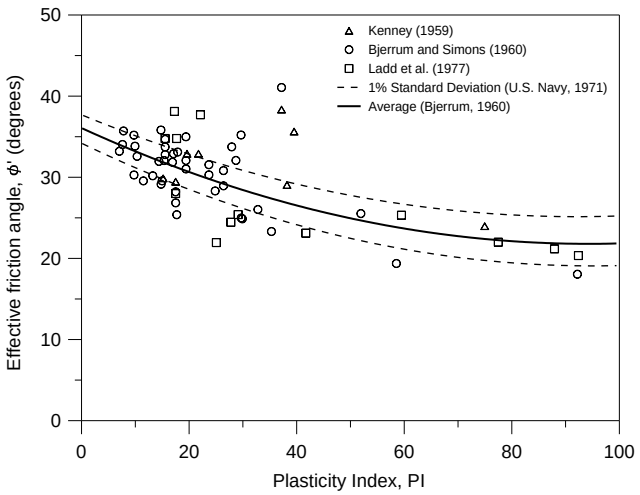

Figure 7 Relationship between PI and φ' (Ashour and Norris, 2000)

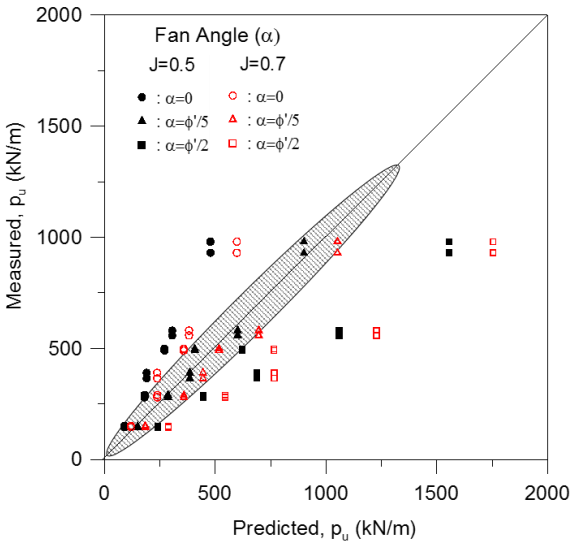

Figure 8 Comparison with various fanning angles (α)

The applying forces on the side and the bottom surface of the wedge are to be classified into two components, such as the shear force and the normal force. The shear forces on the side (F_s) and the bottom surface (F_{sb}) of the wedge can be considered as the lateral friction between pile and soil. The normal force applied to the side and bottom surface is defined as F_n and F_{nb}, respectively. Based on this, the total resistance (F_{tot}) in the loading direction can be determined as following equation by the horizontal force equilibrium;

$$F_{tot} = 2F_s \cos\alpha \sin\theta + F_{sb} \sin\theta + F_{nb} \cos\theta \tag{5}$$

The ultimate soil resistance per unit length (p_u) of soil can be obtained by differentiating F_{tot} with respect to H.

$$\begin{aligned} p_u &= \frac{dF_{tot}}{dH} = 2\cos\alpha \sin\theta \frac{dF_s}{dH} + \sin\theta \frac{dF_{sb}}{dH} + \cos\theta \frac{dF_{nb}}{dH} \\ &= Jc_u D\left[\tan\theta + \frac{1}{\sin\theta} + \sigma_{vo}^{'} + \gamma' H + \frac{\alpha}{\tan\theta}\right] \\ &\quad + Jc_u H\left[2\tan\theta\sin\theta + 2\tan^2\theta\tan\alpha + \frac{2\tan\alpha}{\cos\theta} + 2\cos\theta\right] \\ &\quad + H\tan\alpha\tan\theta\left[2\sigma_{vo}^{'} + \gamma' H\right] \end{aligned} \tag{6}$$

where,

$$\frac{dF_s}{dH} = c_u H \tan\theta \sec\alpha \tag{7}$$

$$\frac{dF_{sb}}{dH} = c_u D\sec\theta + 2c_u H \tan\theta\sec\theta\tan\alpha \tag{8}$$

$$\begin{aligned} \frac{dF_{nb}}{dH} &= \frac{c_u D}{\sin\theta\cos\theta} + \frac{2c_u H\tan\alpha}{\cos^2\theta} + \sigma_{vo}^{'} D\sec\theta + 2\sigma_{vo}^{'} H\tan\alpha\tan\theta\sec\theta \\ &\quad + \gamma' H^2 \tan\alpha\tan\theta\sec\theta + \gamma' HD\sec\theta + 2Hc_u + \frac{\omega c_u D}{\sin\theta} \end{aligned} \tag{9}$$

c_u is the undrained shear strength (kN/m^2), J is the empirical soil constant, which is 0.5 in soft clay (c_u≤20kPa) 0.7 in medium clay (20kPa < c_u≤ 50kPa). β is the pile characteristic length (m^{-1}), where it is expressed as $(K/4E_pI_p)^{1/4}$.

4. RESULT COMPARISONS

Figure 9 shows the proposed and observed p-y characteristics of the field and laboratory test piles. It is found that the proposed p-y curves shows more similarities with the measured value. As shown in Figure 10, the proposed p-y curves for clay soil are tested by comparing with two existing p-y curves which are well known p-y curves, called O'Neill p-y curve (1984) and Matlock p-y curve (1970) for soft clay. The typical p-y characteristics of a test pile, LTP-1 based on pile load tests and predictions using O'Neill (1984) and Matlock (1970) functions are plotted on the same graph. The results by O'Neill and Matlock models show significant differences in the shapes and magnitudes of the ultimate soil resistance per unit length (p_u) compared to the proposed p-y curves by load tests.

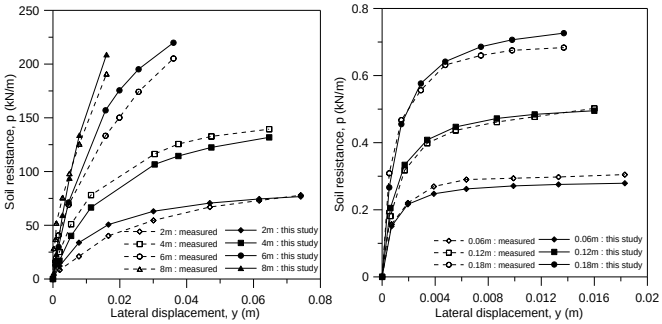

Figure 9 Test results and proposed p-y curves for Incheon marine clay; (a) field load test, (b) laboratory test

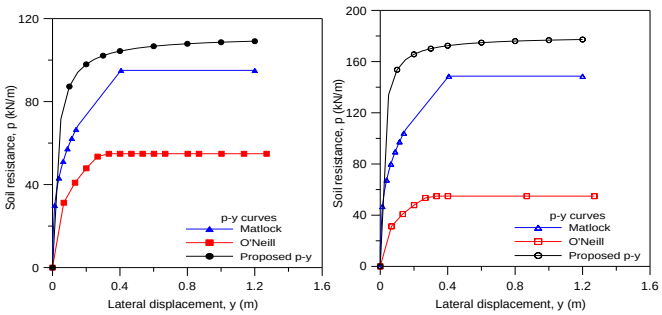

Figure 10 Comparison of p-y curves; (a) depth of two pile diameters, (b) depth of four pile diameters view

The existing models (O'Neill clay model and Matlock soft clay model) have found that different values of initial slope were followed by perfectly plastic behavior. The proposed p-y curve shows the highest ultimate soil resistance, although the initial slope is smaller than the Matlock model. As a result, to obtain detailed information on the behavior of test piles, numerical analysis was performed by a finite difference method (beam-column method). The material properties have accordingly chosen by the field tests (Table 1).

Figure 11 shows the predicted and measured lateral displacement and bending moment profiles in LTP-1. The proposed p-y curves predict well the existing trend of the measured displacement and bending moment when compared with the existing p-y analyses: A reasonably good agreement between the results of proposed p-y curves and the results of the existing p-y curves is obtained to predict the observed ones for the 200kN load. Beyond the 200kN load, the analysis by the existing p-y curves has a considerably larger displacement and bending moment than those by the proposed p-y curves.

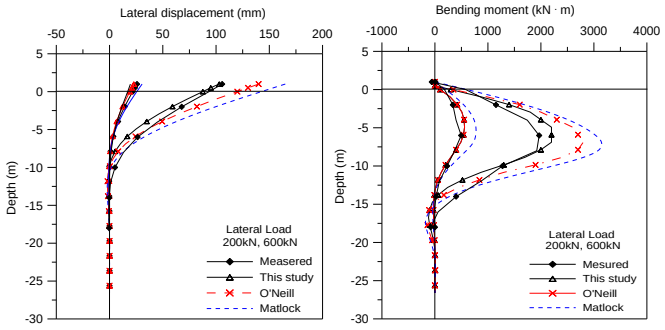

Figure 11 Comparison of predicted results; (a) depth-lateral displacement (LTP-1), (b) depth-bending moment (LTP-1)

5. EFFECT OF PILE-SOIL RIGIDITY

Rigidity between the pile-soil is a direct function of the pile characteristic (rigidity factor; β) and depth (L). Major influence factors are pile diameter (D), and subgrade reaction modulus (K). A series of parametric studies were performed under different soil conditions. The lateral loading – 200kN, 400kN, 600kN, and 800kN – was applied 1m above the ground surface. The pile and soil (soft and medium marine clay) properties used in the parametric study are stated in Table 4 and 5. β and βL for rigid pile in soft clay is 0.076m^{-1}, 1.2. β and βL for rigid pile in medium clay is 0.136m^{-1}, 2.0. β and βL for flexible pile in soft clay is 0.109m^{-1}, 3.3. β and βL for flexible pile in medium clay is 0.193m^{-1}, 5.8.

Table 4 Pile properties : parametric study

	Rigid pile	Flexible pile
Diameter (m)	2.4	1.5
Pile length (m)	15	30
Elastic modulus (kPa)	2.0×10^8	2.0×10^8

Table 5 Pile properties : parametric study

	Soft clay	Medium clay
γ_t (kN/m^3)	17.5	17.5
c_u (kPa)	18	45
ε_{50}	0.02	0.01
ε_{100}	0.06	0.03
K_{avg}	7,000	40,000

The effect of the pile-soil rigidity is investigated for various pile diameters (D) and embedded length (L). As expected, the variation between the calculated and measured pile behavior increased as the characteristic length (βL) increases. Figures 12 and 13 show that the flexible pile in stiff ground (large βL) is more influenced by the various p-y curves than the rigid pile in soft ground (small βL).

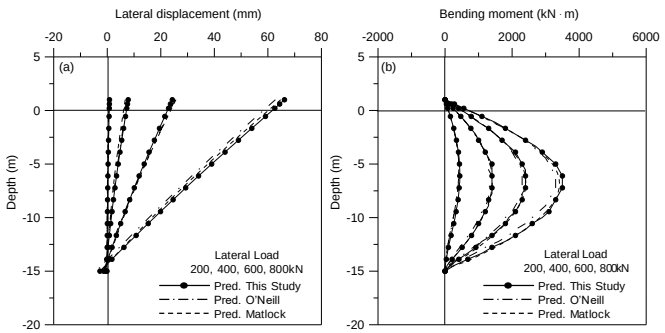

Rigid pile in soft clay (βL = 1.15

Figure 12 (a) lateral displacement (mm), (b) bending moment (kN · m)

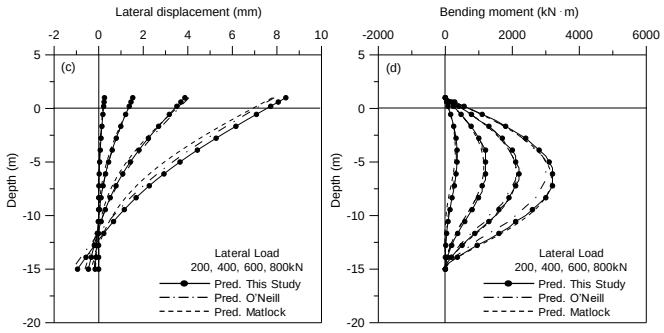

Rigid pile in medium clay (βL = 2.0)

Figure 12 (c) lateral displacement (mm), (d) bending moment (kN · m)

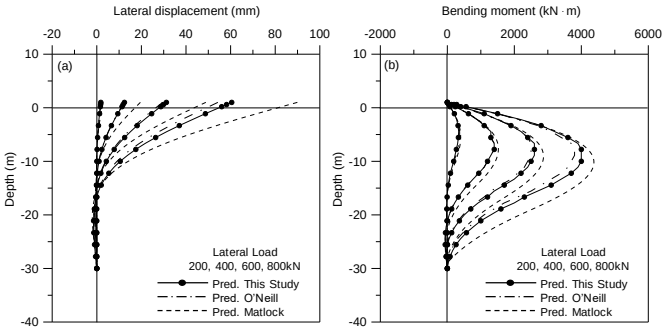

Flexible pile in soft clay (βL = 1.15)

Figure 13 (a) lateral displacement (mm), (b) bending moment (kN · m)

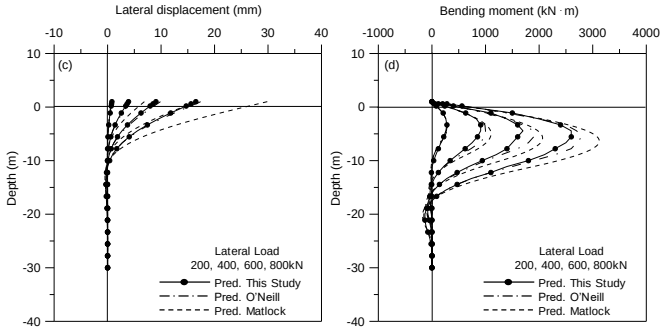

Flexible pile in medium clay (βL = 2.0)

Figure 13 (c) lateral displacement (mm), (d) bending moment (kN · m)

6. CONCLUSIONS

The main objective of this study is to propose an analytical method estimating the behaviour of the laterally loaded drilled shafts embedded in marine clay by considering the various factors influencing lateral soil resistance. Field and laboratory load tests were conducted on Incheon marine clay (western coast of Korea) to observe and determine pile behaviour. Through comparisons with case histories, the proposed p-y curve (function) is found to be in good agreement with in-situ measurements. In addition, the effect of rigidity between the pile-soil was investigated based on parametric study. Based tests and analysis of this study, the following conclusions can be drawn:

1. The analytical methodology to consider soil-pile interaction is proposed based on the 3D wedge failure mode using force equilibrium and effective stress analysis.
2. By taking into account the soil-pile interaction, the p-y function proposed by a nonlinear hyperbolic curve is appropriate and realistic to represent lateral load transfer characteristics of a large

diameter piles in a clay soil. It provides results that are in good agreement with the field test results.

3. The effect of rigidity between the pile-soil was investigated based on parametric study. Based on the calculated results it was found that the flexible pile in stiff ground (large βL) is more influenced by the various p-y curves than the rigid pile in soft ground (small βL). Moreover, the flexible pile was more influenced by various factors compared to rigid piles (rigid pile is nearly unaffected by marine environment).
4. Soil properties on the marine clay have a significant influence on the soil resistance. Therefore, the p-y curves occur depending on the physical soil properties, and it is important to estimate the proper soil properties.

7. ACKNOWLEDGMENTS

This research was supported by Basic Science Research Program through the National Research Foundation of Korea (NRF) funded by the Ministry of Education (No. 2018R1A6A1A08025348), as well as a grant (code19SCIP-B119960-04) from Construction Technology Research Program funded by Ministry of Land, Infrastructure and Transport of Korean government.

8. REFERENCES

Ashford, Scott A., and Teerawut Juirnarongrit (2003). “Evaluation of pile diameter effect on initial modulus of subgrade reaction.” J. Geotech. Geoenvir. Eng., ASCE, 129(3), 234-242.

Ashour, M., and Norris, G. (2000). “Modelling Lateral Soil-Pile Response Based on Soil-Pile Interaction.” J. Geotech. Geoenvir. Eng., ASCE, 126(5), 420-428.

Bowles, J. E. (1996) Foundation anlaysis and design, McGraw-Hill, New York, 1004.

Briaud, J. L., Smith, T.D., and Meyer, B.J. (1983). “Pressuremeter p-y curve design method for laterally loaded piles.” Proceedings of the Geotechnical Engineering Session held in Corpus Christi, ASCE, San Antonio, Texas.

Briaud, J. L. (1997). "SALLOP: Simple approach for lateral loads on piles." J. Geotech. Geoenvir. Eng., ASCE, 123(10), 958–964.

Briaud, J. L., Smith, T., and Mayer, B. (1984). “Laterally loaded piles and the pressuremeter: comparison of existing methods.” Laterally loaded deep foundation. ASTM, West Conshohocken, Pa., 97-111.

Broms, B. (1964). “Lateral Resistance of Piles in Cohesiveness Soils.” J. Soil Mechanics and Foundation Div., ASCE, 90(4), 27-63.

Carter, D. P. (1984). “A non-linear soil model for predicting lateral pile response.” Rep. No. 359, Civil Engineering Dept., Univ. of Auckland, New Zealand.

Jeong, S. S., Kim, Y. H., and Kim, J. Y., (2011). “Influence on lateral rigidity of offshore piles using proposed p-y curves”, Ocean Engineering, 38, 397-408.

Jung, G. J., Kim, D. H., Lee, C. J., and Jeong, S. S., (2017). “Analysis of skin friction behavior in prebored and precast piles based on field loading test”, Journal of Korean Geotechnical Society, **33**: 31-38.

Kim, D. H (2018). “Proposed Shaft Resistance of Prebored and Precast Pile using Field Loading Test”, Doctoral Dissertation, Yonsei University.

Kim, D. H., Park, J. J., Chang, Y. C., and Jeong, S. S. (2018). “Proposed Shear Load-transfer Curves for Prebored and Precast Steel Piles”, *Journal of Korean Geotechnical Society*, Vol.34, No.12, pp. 43–58.

Kim, Y. H. (2010) “Improved lateral load transfer(p-y) curves for large diameter piles based on 3D wedge failure method.” Ph.D. thesis, Yonsei Univ., Seoul.

Liang, R., Shatnawi, E. S., and Nusairat, J. (2007). “Hyperbolic p-y criterion for cohesive soils.” Jordan J. of Civil Eng., 1(1), 38-58

Liang, R., Yang, Ke,, and Nusairat. J. (2007) “p-y criterion for rock mass” J. Geotech. Geoenvir. Eng., Vol. 135(1), pp26-36

Matlock, H. (1970). “Correlations for design of laterally loaded piles in clay.” Paper No. OTC 1204, Proceedings of Second Annual Offshore Technology Conference, Houston, Texas, Vol. 1, 577-594.

Murff, J. D., and Hamilton, J. M. (1993) “P-ultimate for undrained analysis of laterally loaded piles.” Journal of geotechnical engineering, ASCE, 119(1), 91-107

O'Neill, M. W., and Gazioglu. S, M. (1984). “Evaluation of p-y relationships in cohesive soils.” Proceedings of a Analysis and Design of Pile Foundations, ASCE geotechnical Engineering Division, 192-213.

Reese, L.C. (1958). “Discussion of soil modulus for laterally loaded piles.” by B. McClelland and J.A. Focht, Jr., Transactions, ASCE, 123, 1071-1074.

Reese, L. C. (1983). Behavior of piles and pile groups under lateral load, Rep. to the U.S. Dept. of Transportation, Federal Highway Administration, Office of Research, Development, and Technology,Washington, D.C.

Reese, L. C., Cox, W. R., and Koop, F. D. (1975). “Field Testing and Analysis of Laterally Loaded Piles in Stiff Clay”. Proceedings, Offshore Technology Conference, Houston, Texas, Paper No. 2312, 671-690

Reese, L. C., and Welch, R. C. (1975). “Lateral loading of deep foundations in stiff clay.” J. Geotech. Geoenvir. Eng., ASCE, 101(7), 633-649.

Randolph, M. F. (1981). “The response of flexible piles to lateral loading.” Geotechnique, 31(2), 247-259.

Vesic, A. S. (1961). “Bending of beams resting on isotropic elastic solids.” J. Engrg. Mech. Div., ASCE, 87(2), 35-53.

Welch R. C. and Reese L. C. (1972), “Laterally loaded behavior of drilled shafts.” Rep. No. 3-5-65-89, Center from Highway Research, University of Texas, Austin

Yang, K. and Liang, R. (2005). “Lateral response of large diameter drilled shafts in clay.” Proc. 30th Annual Conference on Deep Foundations, Deep Foundation Institute, 115-126.